Advances in Water Resources 62 (2013) 327–339

Contents lists available at ScienceDirect

Advances in Water Resources

journal homepage: www.elsevier.com/locate/advwatres

Velocity and stress jump conditions between a porous medium and a fluid

Francisco J. Valdés-Parada [a], Carlos G. Aguilar-Madera [b], J. Alberto Ochoa-Tapia [a,*], Benoît Goyeau [c]

[a] División de Ciencias Básicas e Ingeniería, Universidad Autónoma Metropolitana-Iztapalapa, Av. San Rafael Atlixco 186, col. Vicentina, 09340 Mexico, Mexico
[b] Instituto Mexicano del Petróleo, Eje Central Lázaro Cardenas no 152, Apartado Postal 14-805 07730 México, D.F., Mexico
[c] Laboratoire EM2C, UPR-CNRS 288, Ecole Centrale Paris, Grande Voie des Vignes, 92295 Châtenay-Malabry, Cedex, France

ARTICLE INFO

Article history:
Available online 23 August 2013

Keywords:
Jump conditions
Closure problem
Momentum transport
Volume averaging

ABSTRACT

Modeling transport phenomena in hierarchical systems can be carried out by either a one domain approach or a two domain approach. The first one involves assuming the system as a pseudo-continuum and is expressed in terms of position-dependent effective medium coefficients. In the two domain approach, the differential equations have position-independent coefficients but require accounting for the corresponding boundary conditions that couple the equations between each homogeneous region. For momentum transport between a porous medium and a fluid, stress boundary conditions have been derived in terms of a jump coefficient that needs to be predicted within a two-domain approach formulation. However, continuity of the velocity is postulated at the dividing surface. In this work, we propose a methodology for the derivation of boundary conditions for both the velocity and the stress. These conditions are expressed in terms of jump coefficients that are computed from the solution of an ancillary macroscopic closure problem. This problem accounts for the deviations from the one and two domain approaches. From the closure problem solution we were also able to determine the position at which the jump conditions should be applied, *i.e.*, the dividing surface position. In addition, we used this methodology adopting the assumptions proposed by Ochoa-Tapia and Whitaker as well as those by Beavers and Joseph. We found that any version of the two domain approach was in agreement with the one domain approach in the bulk of the porous medium and the fluid. However, the same is not true for the process of capturing the essential information of the inter-region.

1. Introduction

Study of momentum transport in channels partially filled with porous media, as the one depicted in Fig. 1, has been a subject of intense theoretical and experimental research over the past 45 years. The motivation for studying this particular configuration relies on the vast variety of applications where this setup can be found. Some examples are: ground water pollution [1]; forest fire modeling [2]; sea water flow above coral reefs [3]; convective oxygen transport from a free fluid through a spherical scaffold of cell culture [4]; among many others. The advent of more sophisticated techniques such as particle image velocimetry has shed new light about transport phenomena near the fluid-porous medium boundary [5]. In addition, computational capabilities have also improved to the point where pore-level simulations can be carried out using the Lattice-Boltzmann method to estimate the drastic variations of the velocity taking place at this boundary [6]. Despite these remarkable advances, most practical applications require accounting for volume averaged velocities and thus the need for developing theoretical schemes that lead to reliable predictions of these fields. The method of volume averaging [7] is an upscaling technique in which the essential information from the pore scale is captured in macroscale equations. These equations arise from properly averaging the governing equations at the pore scale and imposing a set of reasonable assumptions, which can be regarded as scaling postulates [8]. For momentum transport in the bulk of porous media, Stokes or Navier–Stokes equations are upscaled leading to the Darcy's equation or one of its extension (involving Brinkman and/or Forchheimer correction terms) [9,10].

For configurations partially occupied by a porous region, the problematic related to the scale separation remains but it is combined with the challenging description of average momentum in the interfacial region (inter-region). Two approaches have been used and compared in the literature: the *one- or the two-domain approaches* [11]. In the one-domain approach (ODA) the fluid-porous system is assumed as a pseudo-continuum where momentum transport is governed by a generalized transport equation (GTE), free of length-scale constraints, and valid both in the homogeneous fluid and porous regions but also in the thin transition inter-region

* Corresponding author. Tel.: +52 5558044642.
E-mail address: jaot@xanum.uam.mx (J.A. Ochoa-Tapia).

0309-1708/$ - see front matter © 2013 Elsevier Ltd. All rights reserved.
http://dx.doi.org/10.1016/j.advwatres.2013.08.008

Nomenclature

$b_{\alpha\lambda}$	closure variable that maps $\frac{d\langle v_\beta\rangle^\beta_\lambda}{dy}\Big\|_{y_0}$ onto $\hat{v}_\alpha$ $(\alpha,\lambda=\eta,\omega)$, m
$\mathbf{g}$	gravity vector, m/s^2
K_β	position-dependent permeability coefficient, m^2
$K_{\beta\omega}$	permeability coefficient in the homogeneous porous medium, m^2
ℓ	characteristic size of a unit cell in the porous medium bulk, m
ℓ_σ	characteristic size of the σ-phase, m
L_α	characteristic length of the homogeneous α-region $(\alpha=\eta,\omega)$, m
p_β	total pressure in the β-phase, Pa
$\langle p_\beta\rangle^\beta$	intrinsic average of the pressure for the one-domain approach, Pa
$\langle p_\beta\rangle^\beta_\alpha$	intrinsic average of the pressure in the α-region $(\alpha=\eta,\omega)$ for the two-domain approach, Pa
r_0	characteristic size of the averaging domain, m
$s_{\alpha\lambda}$	closure variable that maps $\langle v_\beta\rangle^\beta_\lambda\Big\|_{y_0}$ onto $\hat{v}_\alpha$ $(\alpha,\lambda=\eta,\omega)$
U	dimensionless velocity corresponding to the one-domain approach
U_α	dimensionless velocity corresponding to the two-domain approach $(\alpha=\eta,\omega)$
$\mathbf{v}_\beta$	velocity vector in the β-phase, m/s
$\langle v_\beta\rangle^\beta$	intrinsic averaged velocity for the one-domain approach, m/s
$\langle v_\beta\rangle^\beta_\alpha$	intrinsic averaged velocity in the α-region $(\alpha=\eta,\omega)$ for the two-domain approach, m/s
$\langle v_\beta\rangle^\beta_{\omega,\infty}$	intrinsic velocity value at the porous medium bulk, m/s
$\hat{v}_\alpha$	macroscopic deviations of the velocity in the α-region $(\alpha=\eta,\omega)$, m/s
$\mathscr{V}_\alpha$	portion occupied by the α-region $(\alpha=\eta,\omega)$ within the large-scale averaging domain, m^3
$\mathscr{V}_\infty$	large-scale averaging domain, m^3
x	horizontal coordinate, m
y	vertical coordinate, m
y_0	position of the dividing surface, m
y_α	horizontal boundaries of the inter-region $(\alpha=\eta,\omega)$, m

Greek symbols

α	jump coefficient in the original Beavers and Joseph boundary condition
$\alpha_{\eta\omega}$	jump coefficient in the stress difference for the first jump condition, m
β	jump coefficient in the original Ochoa-Tapia and Whitaker boundary condition
$\beta_{\omega\eta}$	jump coefficient for the velocity difference in the second boundary condition
ε_β	position-dependent porosity coefficient
$\varepsilon_{\beta\omega}$	porosity coefficient in the homogeneous porous medium
μ_β	viscosity coefficient in the β-phase, Pa s
ϑ	jump coefficient in the velocity difference for the first jump condition
ϖ	jump coefficient in the stress difference for the second jump condition
ρ_β	density of the β-phase, kg/m^3

(see Fig. 2(a)) where the effective coefficients (permeability, porosity) are continuously space-dependent [12–14]. This representation is particularly adapted for numerical simulations where the main difficulty concerns the spatial discretization within the inter-region.

The two-domain approach (TDA), based on the idea that the porous region is homogeneous up to a "virtual" dividing surface, requires boundary conditions for the coupling of the governing equations in the homogeneous regions (Fig. 2(b)). The importance of the dividing surface position has also been recently acquainted by several authors [15,14,16]. In the pioneering study proposed by Beavers and Joseph [17], a Stokes flow in the fluid channel is coupled to the Darcy's law in the homogeneous porous layer by using the well known semi-empirical slip boundary condition

$$\left.\frac{d\langle v_\beta\rangle^\beta_\eta}{dy}\right|_{y_0}=\frac{\alpha}{\sqrt{K_{\beta\omega}}}\left(\langle v_\beta\rangle^\beta_\eta\Big|_{y_0}-\varepsilon_{\beta\omega}\langle v_\beta\rangle^\beta_\omega\Big|_{y_0}\right) \tag{1}$$

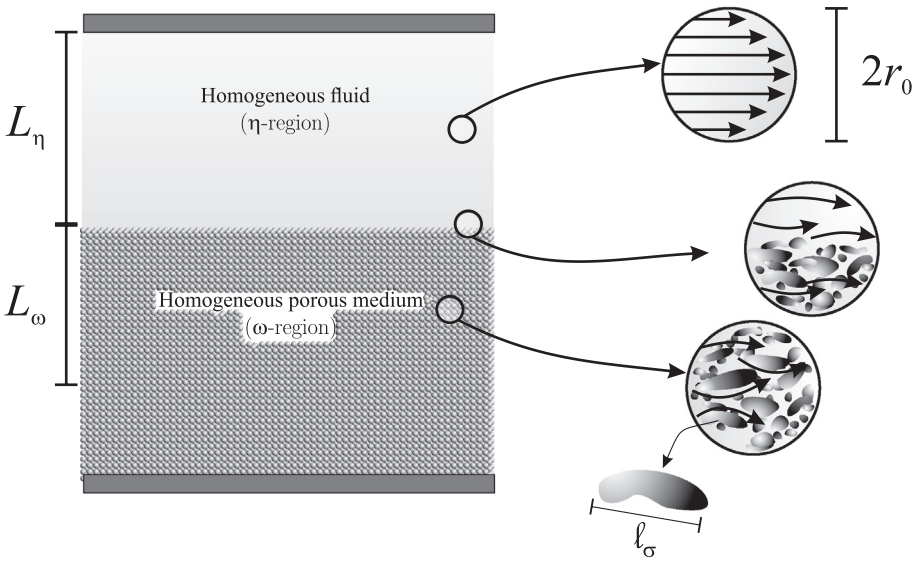

Fig. 1. Sketch of the system including characteristic lengths.

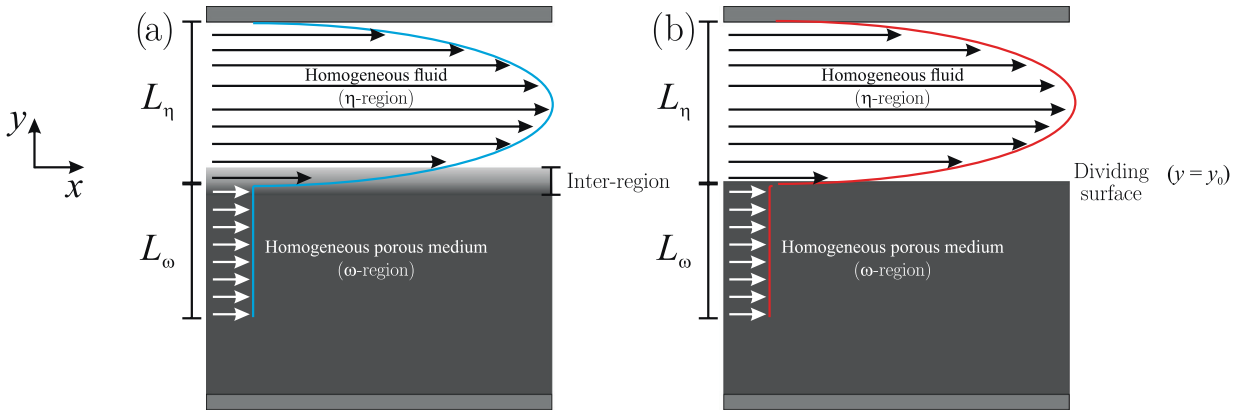

Fig. 2. Sketches of the domains and velocity profiles for (a) the one-domain approach and (b) the two-domain approach.

where α is an adjustable jump coefficient that depends of the local geometry of the interfacial region. This jump condition has been avoided through the use of Brinkman extension to Darcy's law in the porous region [18–20]. In that case, continuity of both the velocity and the stress were imposed in order to couple the momentum equations in the fluid and in the porous layer. In fact, it is worth mentioning that the length-scale constraints used for the derivation of the macroscopic equations in both homogeneous regions are not satisfied in the interfacial region. This difficulty has been tackled in the context of volume averaging by assuming continuity of the velocity at the dividing surface and deriving a stress jump boundary condition [12,21] which takes the form:

$$\left.\frac{d\langle v_\beta\rangle_\omega^\beta}{dy}\right|_{y_0} - \left.\frac{d\langle v_\beta\rangle_\eta^\beta}{dy}\right|_{y_0} = \frac{\varepsilon_{\beta\omega}\beta}{\sqrt{K_{\beta\omega}}}\langle v_\beta\rangle_\omega^\beta\Big|_{y_0} \tag{2}$$

In condition (2), β is the stress jump coefficient, which is also dependent on the local geometry and the location of the interface. This coefficient has been recently predicted through different methodologies [11,22,13,15,14,23].

It should be stressed that, in practice, the two-domain approach is the most widely used modeling choice for several reasons, such as: (i) All the differential equations are written in terms of coefficients that are constants in position, (ii) Since there is no inter-region in this approach, there is no need to account for the rapid variations of properties (such as porosity, permeability, etc.) in this part of the system. As consequence, the numerical solution of the TDA is computationally less expensive than solving the ODA. (iii) Relevant transport phenomena taking place in the inter-region in the ODA are incorporated in the boundary conditions for the TDA at the dividing surface. Despite these attractive features, several questions remain to be addressed: *is the continuity of the velocity relevant? What is the physical meaning of the jump conditions? Where is the dividing surface located? What is the relation between the dividing surface and the inter-region?* The objective of this work is to address these questions. We thus propose a methodology to derive the jump conditions for both the velocity and the stress. This methodology is based on the introduction of *macroscopic velocity deviations* [7] whose integral over the transition layer leads to a jump condition for the velocity fields while similar integration of the governing equations for the macroscopic velocity deviations gives rise to the stress jump condition [12]. Note that the integrals of these deviations have been previously identified, in the context of matched asymptotic expansion method, as excess quantities [22,15,14].

The manuscript is organized as follows. The local and the macroscopic one and two-domain momentum equations are presented in Section 2 while the boundary conditions at the dividing surface are derived Section 3. The present analysis is applied to the Beavers and Joseph (Section 4) and Ochoa-Tapia and Whitaker (Section 5) cases where the position of the dividing surface and the jump coefficients are determined. The different models are quantitatively compared in term of velocity profiles in Section 6. Section 7 is devoted to the concluding remarks.

2. Microscopic and macroscopic governing equations

Consider the system sketched in Fig. 1, consisting of a channel that is partially filled with a porous medium [17]. For the sake of simplicity we adopt the following assumptions:

- The porous medium is rigid and homogeneous. The solid phase is hereby denoted as the σ-phase.
- The fluid phase (*i.e.* the β-phase) passing above the porous medium also saturates it.
- The fluid is assumed to be Newtonian and incompressible.
- Inertial effects are assumed to be negligible compared with viscous drag.
- Transport process is assumed to take place under steady state conditions.

Under these circumstances, the governing equations for mass and momentum transport at the pore-scale are given by

$$\nabla\cdot\mathbf{v}_\beta = 0, \quad \text{in the } \beta-\text{phase} \tag{3}$$

$$0 = -\nabla p_\beta + \rho_\beta\mathbf{g} + \mu_\beta\nabla^2\mathbf{v}_\beta, \quad \text{in the } \beta-\text{phase} \tag{4}$$

In addition, non-slip conditions are enforced at the solid–fluid interface. Since we are not interested in solving the pore-scale equations, we use the method of volume averaging to derive upscaled models that capture the essential features of the microscale transport. This is achieved by averaging the pore-scale equations within an averaging domain $\mathscr{V}$ (with norm V) and imposing some reasonable assumptions that allow keeping the non-redundant information. The characteristic length of the averaging domain is denoted by r_0 and it is usually bounded to be sufficiently large (with respect to the characteristic length at the microscale, *eg.*, ℓ_σ) to capture the essential features of the pore-scale and, at the same time, sufficiently small with respect to the characteristic lengths of the macroscale (*i.e.*, L_η, L_ω) to avoid losing too much information in the averaging process (see Fig. 1) (the reader interested in a detailed description of the development of the length-scale constraints in the averaging process is directed to Refs. [24,25]). The derivation of the one- and two-domain approaches using the method of vol-

ume averaging is available elsewhere [12,13]; here we only present the resulting models. The one-domain approach (see Fig. 2(a)) is given by

$$0 = -\frac{d\langle p_\beta\rangle^\beta}{dx} + \mu_\beta \frac{d^2\langle v_\beta\rangle^\beta}{dy^2} + \left(\mu_\beta \varepsilon_\beta^{-1}\frac{d^2\varepsilon_\beta}{dy^2}\right)\langle v_\beta\rangle^\beta - \mu_\beta \varepsilon_\beta^{-1}\frac{d\varepsilon_\beta}{dy} \times \frac{d\langle v_\beta\rangle^\beta}{dy} - \mu_\beta K_\beta^{-1}\varepsilon_\beta\langle v_\beta\rangle^\beta \quad (5)$$

Here we have limited our study to the fully-developed, steady, one-dimensional flow process studied by BJ [17], so that the only non-zero component of the volume-averaged velocity vector is the one that is parallel to the horizontal boundaries (*i.e.*, the x-component of the volume-averaged velocity, Fig. 2). In Eq. (5), $\langle p_\beta\rangle^\beta$ and $\langle v_\beta\rangle^\beta$, denote the intrinsic averaged pressure and velocity, respectively. These quantities are related to their surface-averaged counterparts by means of the identity: $\langle\psi_\beta\rangle = \varepsilon_\beta\langle\psi_\beta\rangle^\beta$ $(\psi_\beta = p_\beta, v_\beta)$; with ε_β being the volume fraction of the β-phase within the averaging domain (*i.e.*, $\varepsilon_\beta = V_\beta/V$). Finally, K_β represents a position-dependent permeability coefficient. For the process under consideration, all quantities involved in Eq. (5) (with the exception of the fluid viscosity, μ_β) are position-dependent only in the vertical direction (*i.e.*, the y-direction, see Fig. 2). The computation of the spatial variations of ε_β is available from (see Appendix C therein [13]) and consisted on numerically determining the values of $\langle 1\rangle$ at several positions around the boundary of a fluid and a porous medium. For the sake of simplicity, the porous medium was modeled as a periodic and isotropic array of spherical particles in cubic unit cells. The numerical results were approximated by the following algebraic expression,

$$\varepsilon_\beta = \begin{cases} 1, & \text{in the } \eta-\text{ region} \\ \frac{1}{2}(\varepsilon_{\beta\omega}+1)+\frac{1}{4}(\varepsilon_{\beta\omega}-1)\left(\frac{y}{r_0}\right)\left[\left(\frac{y}{r_0}\right)^2-3\right], & \text{in the inter }-\text{ region} \\ \varepsilon_{\beta\omega}, & \text{in the } \omega\ -\text{ region} \end{cases} \quad (6a)$$

In the above expression, the subscript ω indicates that the quantity corresponds to the homogeneous ω-region. In addition, the spatial variations of K_β were determined by solving the corresponding closure problems in the inter-region using unit cells containing variable amounts of the porous medium (modeled as an array of in-line squares [23] and cubes [26]) and the fluid. In this case, the numerical results were fitted using the following expression,

$$K_\beta^{-1} = \begin{cases} 0, & \text{in the } \eta-\text{ region} \\ K_{\beta\omega}^{-1}\left(c_0+\sum_{i=1}^{3} c_i \exp\left[-\left(\frac{y}{r_0}-t_0\right)t_i^{-1}\right]\right), & \text{in the inter }-\text{ region} \\ K_{\beta\omega}^{-1}, & \text{in the } \omega\ -\text{ region} \end{cases} \quad (6b)$$

In Eq. (6b), the values of the parameters c_i and t_i $(i = 0,\ldots,3)$ are available for two-dimensional (see Table 1 in Ref. [23]) and three-dimensional (see Table 2 in Ref. [26]) unit cells. It should be stressed that in the statistical fittings provided in Eqs. (6) the correlation coefficient was above 0.99 in all cases.

Table 1
Dependent variables and sources for the closure problems involved in this work.

Source	i	$f_{\lambda i}$		$\Psi_{\lambda i}$		This work	
		$\lambda=\eta$	$\lambda=\omega$	$\lambda=\eta$	$\lambda=\omega$	ψ_i	Γ_i
$\langle v_\beta\rangle_\omega^\beta\big\vert_{y_0}$	1	$s_{\eta\omega}$	$s_{\omega\omega}$	0	$-(M_\beta+\varepsilon_{\beta\omega}K_{\beta\omega}^{-1})$	−1	0
$\langle v_\beta\rangle_\eta^\beta\big\vert_{y_0}$	2	$s_{\eta\eta}$	$s_{\omega\eta}$	$-M_\beta$	0	1	0
$\frac{d\langle v_\beta\rangle_\eta^\beta}{dy}\big\vert_{y_0}$	3	$b_{\eta\eta}$	$b_{\omega\eta}$	$\frac{d\ln\varepsilon_\beta}{dy}$	0	0	1
$\frac{d\langle v_\beta\rangle_\omega^\beta}{dy}\big\vert_{y_0}$	4	$b_{\eta\omega}$	$b_{\omega\omega}$	0	$\frac{d\ln\varepsilon_\beta}{dy}$	0	−1

Table 2
Position of the dividing surface and jump coefficients involved in the TDA for several porosity values.

$\varepsilon_{\beta\omega}$	y_0/r_0	ϑ	α	$\alpha_{\eta\omega}$	ϖ	β	$\beta_{\omega\eta}$
0.3	1.020	807.4	0.0265	0.0768	0.992	−1253.47	-2.71×10^{-14}
0.4	1.020	506.1	0.0341	0.0805	0.959	−1156.27	-1.82×10^{-14}
0.5	1.025	328.5	0.0425	0.0920	0.963	−968.41	1.37×10^{-13}
0.6	1.025	172.7	0.0598	0.0964	0.966	−812.40	-4.52×10^{-15}
0.7	1.025	93.1	0.0841	0.1029	0.969	−708.47	-5.62×10^{-13}
0.8	1.025	68.6	0.0976	0.1341	0.972	−675.81	-5.11×10^{-13}
0.9	1.025	46.8	0.1180	0.1689	0.977	−796.16	-3.33×10^{-13}

The two-domain approach involves using volume-averaged expressions in each homogeneous region and coupling them with appropriate boundary conditions at the dividing surface. As shown in Fig. 2, the position of the dividing surface is denoted by y_0. In addition, $y = 0$ is located at the position in which $\varepsilon_\beta = (\varepsilon_\eta + \varepsilon_\omega)/2$. In general, it is not necessary true that $y_0 = 0$.

For the case here studied, the governing equations in each region correspond to the Stokes-equation and the Darcy–Brinkman equation,

$$0 = -\frac{d\langle p_\beta\rangle_\eta^\beta}{dx} + \mu_\beta\frac{d^2\langle v_\beta\rangle_\eta^\beta}{dy^2}, \quad \text{in the } \eta-\text{region} \quad (7a)$$

$$0 = -\frac{d\langle p_\beta\rangle_\omega^\beta}{dx} + \mu_\beta\frac{d^2\langle v_\beta\rangle_\omega^\beta}{dy^2} - \mu_\beta\varepsilon_{\beta\omega}K_{\beta\omega}^{-1}\langle v_\beta\rangle_\omega^\beta, \quad \text{in the } \omega-\text{ region} \quad (7b)$$

Contrary to the ODA, all the coefficients involved in these equations are constants. Furthermore, from Ref. [26], we have the following relation between permeability and porosity for 3D unit cells consisting of arrays of in-line cubes,

$$\frac{K_{\beta\omega}}{\ell^2} = 1.606\times10^{-4} + 2.047\times10^{-5}\exp(8.397\varepsilon_{\beta\omega}) \quad (8)$$

with ℓ being the characteristic length of a unit cell.

For the sake of simplicity, in this work, we constrain the analysis from the bulk of the porous medium ($y = -L_\omega$) to the upper wall ($y = L_\eta$) shown in Fig. 1. Imposing Darcy's law and the non-slip condition at these boundaries, we have

$$y = -L_\omega, \quad \langle v_\beta\rangle_{\omega,\infty}^\beta = -\frac{K_{\beta\omega}}{\mu_\beta\varepsilon_{\beta\omega}}\frac{d\langle p_\beta\rangle_\omega^\beta}{dx} \quad (9a)$$

$$y = L_\eta, \quad \langle v_\beta\rangle_\eta^\beta = 0 \quad (9b)$$

Indeed, these are the only necessary boundary condition for solving the ODA. However, this is not the case for the TDA where two more boundary conditions are required at the dividing surface ($y = y_0$). These conditions, as well as the dividing surface position, are derived in the following paragraphs.

Before moving on, we note that, for the type of flow and system studied by BJ [17], it is reasonable to assume a constant pressure gradient everywhere in the system; this is

$$\frac{d\langle p_\beta\rangle^\beta}{dx} = \frac{d\langle p_\beta\rangle_\eta^\beta}{dx} = \frac{d\langle p_\beta\rangle_\omega^\beta}{dx} = -\frac{\mu_\beta\varepsilon_{\beta\omega}}{K_{\beta\omega}}\langle v_\beta\rangle_{\omega,\infty}^\beta \quad (10)$$

In this way, the differential equations for the ODA and TDA take the form

ODA

$$0=\frac{d^2\langle v_\beta\rangle^\beta}{dy^2}-\varepsilon_\beta^{-1}\frac{d\varepsilon_\beta}{dy}\frac{d\langle v_\beta\rangle^\beta}{dy}+\left(\varepsilon_\beta^{-1}\frac{d^2\varepsilon_\beta}{dy^2}-\varepsilon_\beta K_\beta^{-1}\right)\langle v_\beta\rangle^\beta+\varepsilon_{\beta\omega}K_{\beta\omega}^{-1}\langle v_\beta\rangle^\beta_{\omega,\infty}\quad\forall y\in(-L_\omega,L_\eta)\tag{11}$$

TDA

$$0=\frac{d^2\langle v_\beta\rangle^\beta_\eta}{dy^2}+\varepsilon_{\beta\omega}K_{\beta\omega}^{-1}\langle v_\beta\rangle^\beta_{\omega,\infty},\quad\forall y\in(y_0,L_\eta)\tag{12a}$$

$$0=\frac{d^2\langle v_\beta\rangle^\beta_\omega}{dy^2}-\varepsilon_{\beta\omega}K_{\beta\omega}^{-1}\left(\langle v_\beta\rangle^\beta_\omega-\langle v_\beta\rangle^\beta_{\omega,\infty}\right),\quad\forall y\in(-L_\omega,y_0)\tag{12b}$$

From the above formulations, it is evident that the expressions for the one and two domain approaches are equal in the homogeneous regions of the system. It suffices to regard ε_β as a constant in Eq. (11) and take into account the limits given in Eq. (6) to recover Eq. (12).

3. Boundary conditions at the dividing surface

As shown in Fig. 2(a), there is a zone of changes that separates one homogeneous region from another, *i.e.*, the inter-region. In previous works [13,23] we have established that the zone where ε_β and K_β exhibit changes is the same and it is on the order of $2r_0$. With r_0 being ten times the length of a unit cell in the bulk of the porous medium, *i.e.*, $r_0=10\ell$. However, this is not necessarily extensive to the zone where the difference between the velocity fields from the ODA and TDA is not negligible. With the aim of quantifying this difference, let us define the macroscopic velocity deviations as

$$\hat{v}_\lambda=\langle v_\beta\rangle^\beta-\langle v_\beta\rangle^\beta_\lambda,\lambda=\omega,\eta\tag{13}$$

This concept is similar to the temperature macroscopic deviations involved in the derivation of local-thermal equilibrium models (see Chap. 2 in Ref. [7]). Certainly, $\hat{v}_\lambda=0$ ($\lambda=\omega,\eta$) in the homogeneous regions.

The fact that the macroscopic velocity deviations are non-zero in the inter-region follows from the use of the TDA inside of this boundary region. In general, it is unavoidable to have non-zero values of the macroscopic deviations fields within the inter-region. For this reason, in the following paragraphs we derive and formally solve the boundary-value problem governing the fields of the macroscopic velocity deviations. We refer to this problem as the *macroscopic closure problem*. As will be shown afterwards, accounting for the fields of the macroscopic deviations is essential for the derivation of the jump conditions.

3.1. Macroscopic closure problem

From the above, it is clear that the derivation and solution of the boundary-value problem for the macroscopic deviations is in order. To this end, we have from Eq. (13) that the governing equations for the macroscopic deviations arise from subtracting Eq. (12) to Eq. (11); the resulting expressions are

$$0=\frac{d^2\hat{v}_\eta}{dy^2}-\varepsilon_\beta^{-1}\frac{d\varepsilon_\beta}{dy}\frac{d\hat{v}_\eta}{dy}+\left(\varepsilon_\beta^{-1}\frac{d^2\varepsilon_\beta}{dy^2}-\varepsilon_\beta K_\beta^{-1}\right)\hat{v}_\eta-\varepsilon_\beta^{-1}\frac{d\varepsilon_\beta}{dy}\frac{d\langle v_\beta\rangle^\beta_\eta}{dy}+\left(\varepsilon_\beta^{-1}\frac{d^2\varepsilon_\beta}{dy^2}-\varepsilon_\beta K_\beta^{-1}\right)\langle v_\beta\rangle^\beta_\eta\quad\forall y\in\left(y_0,y_\eta\right)\tag{14a}$$

$$0=\frac{d^2\hat{v}_\omega}{dy^2}-\varepsilon_\beta^{-1}\frac{d\varepsilon_\beta}{dy}\frac{d\hat{v}_\omega}{dy}+\left(\varepsilon_\beta^{-1}\frac{d^2\varepsilon_\beta}{dy^2}-\varepsilon_\beta K_\beta^{-1}\right)\hat{v}_\omega-\varepsilon_\beta^{-1}\frac{d\varepsilon_\beta}{dy}\frac{d\langle v_\beta\rangle^\beta_\omega}{dy}+\left(\varepsilon_\beta^{-1}\frac{d^2\varepsilon_\beta}{dy^2}-\varepsilon_\beta K_\beta^{-1}+\varepsilon_{\beta\omega}K_{\beta\omega}^{-1}\right)\langle v_\beta\rangle^\beta_\omega\quad\forall y\in(-y_\omega,y_0)\tag{14b}$$

With the aim of localizing the terms involving the velocity and its derivatives in the above expressions at y_0, we propose the following Taylor series expansions around the position of the dividing surface:

$$\langle v_\beta\rangle^\beta_\lambda\Big|_y=\langle v_\beta\rangle^\beta_\lambda\Big|_{y_0}+\Delta y\frac{d\langle v_\beta\rangle^\beta_\lambda}{dy}\Big|_{y_0}+\frac{(\Delta y)^2}{2}\frac{d^2\langle v_\beta\rangle^\beta_\lambda}{dy^2}\Big|_{y_0}+\cdots\quad\lambda=\omega,\eta\tag{15a}$$

$$\frac{d\langle v_\beta\rangle^\beta_\lambda}{dy}\Big|_y=\frac{d\langle v_\beta\rangle^\beta_\lambda}{dy}\Big|_{y_0}+\Delta y\frac{d^2\langle v_\beta\rangle^\beta_\lambda}{dy^2}\Big|_{y_0}+\frac{(\Delta y)^2}{2}\frac{d^3\langle v_\beta\rangle^\beta_\lambda}{dy^3}\Big|_{y_0}+\cdots\quad\lambda=\omega,\eta\tag{15b}$$

here $\Delta y=y-y_0$. As a first approximation, we propose to use only the zeroth-order terms in the above expansions. Under these circumstances we may write Eq. (14) as follows

$$0=L(\hat{v}_\eta)\underbrace{-\varepsilon_\beta^{-1}\frac{d\varepsilon_\beta}{dy}\frac{d\langle v_\beta\rangle^\beta_\eta}{dy}\Big|_{y_0}}_{\text{source}}\underbrace{+M_\beta\langle v_\beta\rangle^\beta_\eta\Big|_{y_0}}_{\text{source}}\quad\forall y\in\left(y_0,y_\eta\right)\tag{16a}$$

$$0=L(\hat{v}_\omega)\underbrace{-\varepsilon_\beta^{-1}\frac{d\varepsilon_\beta}{dy}\frac{d\langle v_\beta\rangle^\beta_\omega}{dy}\Big|_{y_0}}_{\text{source}}\underbrace{+\left(M_\beta+\varepsilon_{\beta\omega}K_{\beta\omega}^{-1}\right)\langle v_\beta\rangle^\beta_\omega\Big|_{y_0}}_{\text{source}}\quad\forall y\in(-y_\omega,y_0)\tag{16b}$$

For simplicity, we used the definitions

$$L(\cdot)=\left\{\frac{d^2}{dy^2}-\varepsilon_\beta^{-1}\frac{d\varepsilon_\beta}{dy}\frac{d}{dy}+M_\beta\right\}(\cdot)\tag{17a}$$

$$M_\beta=\varepsilon_\beta^{-1}\frac{d^2\varepsilon_\beta}{dy^2}-K_\beta^{-1}\varepsilon_\beta\tag{17b}$$

In this way, the velocities and their derivatives are constant sources in the macroscopic closure problem. As explained above, outside the region comprised in $y\in(-y_\omega,y_\eta)$ the macroscopic deviations are null. We may thus impose the following boundary conditions,

$$\text{at } y=y_\eta\quad\hat{v}_\eta=0;\quad\frac{d\hat{v}_\eta}{dy}=0\tag{18a}$$

$$\text{at } y=-y_\omega,\quad\hat{v}_\omega=0;\quad\frac{d\hat{v}_\omega}{dy}=0\tag{18b}$$

Certainly, only two of these four boundary conditions are necessary in order to solve the macroscopic closure problem. As will be shown later, the remaining two boundary conditions are necessary to determine the width of the zone where the macroscopic deviations are non-zero as well as the dividing surface position, y_0.

In order to complete the macroscopic closure problem statement, it is necessary to impose boundary conditions at $y=y_0$. To this end, we take into account the fact that the velocity and stress from the ODA are continuous at this boundary, *i.e.*,

$$\text{at } y_0, \quad \langle v_\beta\rangle^\beta\Big|_{y_0^-} = \langle v_\beta\rangle^\beta\Big|_{y_0^+} \tag{19a}$$

$$\text{at } y_0, \quad \mu_\beta \frac{d\langle v_\beta\rangle^\beta}{dy}\Big|_{y_0^-} = \mu_\beta \frac{d\langle v_\beta\rangle^\beta}{dy}\Big|_{y_0^+} \tag{19b}$$

Substitution of the decomposition given by Eq. (13), yields

$$\text{at } y_0, \quad \hat{v}_\omega + \underbrace{\langle v_\beta\rangle^\beta_\omega\Big|_{y_0}}_{\text{source}} = \hat{v}_\eta + \underbrace{\langle v_\beta\rangle^\beta_\eta\Big|_{y_0}}_{\text{source}} \tag{20a}$$

$$\text{at } y_0, \quad \frac{d\hat{v}_\omega}{dy} + \underbrace{\frac{d\langle v_\beta\rangle^\beta_\omega}{dy}\Big|_{y_0}}_{\text{source}} = \frac{d\hat{v}_\eta}{dy} + \underbrace{\frac{d\langle v_\beta\rangle^\beta_\eta}{dy}\Big|_{y_0}}_{\text{source}} \tag{20b}$$

In this way, the macroscopic closure problem is given by the differential equations (16), which are subject to the boundary conditions in Eq. (18) and (20). As will be shown below, for the derivation of the jump boundary conditions it is also necessary that the macroscopic deviations also satisfy the two integral constraints given later in Section 3.2. Due to the linearity of this boundary-value problem, we may apply the superposition principle and propose the following solutions in terms of the constant sources

$$\hat{v}_\omega = s_{\omega\eta}\langle v_\beta\rangle^\beta_\eta\Big|_{y_0} + s_{\omega\omega}\langle v_\beta\rangle^\beta_\omega\Big|_{y_0} + b_{\omega\eta}\frac{d\langle v_\beta\rangle^\beta_\eta}{dy}\Big|_{y_0} + b_{\omega\omega}\frac{d\langle v_\beta\rangle^\beta_\omega}{dy}\Big|_{y_0} \tag{21a}$$

$$\hat{v}_\eta = s_{\eta\eta}\langle v_\beta\rangle^\beta_\eta\Big|_{y_0} + s_{\eta\omega}\langle v_\beta\rangle^\beta_\omega\Big|_{y_0} + b_{\eta\eta}\frac{d\langle v_\beta\rangle^\beta_\eta}{dy}\Big|_{y_0} + b_{\eta\omega}\frac{d\langle v_\beta\rangle^\beta_\omega}{dy}\Big|_{y_0} \tag{21b}$$

where $s_{\omega\eta}$, $s_{\omega\omega}$, $s_{\eta\eta}$, $s_{\eta\omega}$, $b_{\omega\eta}$, $b_{\omega\omega}$, $b_{\eta\eta}$ and $b_{\eta\omega}$ are macroscopic closure variables that solve specific boundary-value problems. These problems can be condensed into the following one (in all equations $i = 1, 2, 3$ or 4)

$$\text{at } y = y_\eta, \quad f_{\eta i} = 0; \quad \frac{df_{\eta i}}{dy} = 0 \tag{22a}$$

$$L(f_{\eta i}) = \Psi_{\eta i}, \quad y \in (y_0, y_\eta) \tag{22b}$$

$$\text{at } y = y_0, \quad f_{\omega i} = f_{\eta i} + \psi_i \tag{22c}$$

$$\text{at } y = y_0, \quad \frac{df_{\omega i}}{dy} = \frac{df_{\eta i}}{dy} + \Gamma_i \tag{22d}$$

$$L(f_{\omega i}) = \Psi_{\omega i}, \quad y \in (-y_\omega, y_0) \tag{22e}$$

$$\text{at } y = -y_\omega, \quad f_{\omega i} = 0; \quad \frac{df_{\omega i}}{dy} = 0 \tag{22f}$$

The dependent variables, $f_{\lambda i}$ and sources, $\Psi_{\lambda i}$, ψ_i, Γ_i, for each problem are available in Table 1. These closure problems were numerically solved using finite differences involving sufficient mesh elements so that the solution was independent of the numerical parameters. In the following paragraphs we will present the role played by these closure variables in the computation of the coefficients involved in the jump conditions.

3.2. Jump conditions

At this point it is worth emphasizing that the macroscopic deviations represent the errors induced by using the fields of the TDA outside from their domain of validity. These errors are corrected by means of the jump boundary conditions. In other words, the purpose of the jump conditions is to amend for the errors induced from using the TDA in the inter-region by ensuring that the ODA is satisfied *on the average* [12] in this part of the system. This is the key feature of the jump conditions and we propose two average constraints to accomplish this goal:

First integral constraint:
Require that the average of the differences of the velocity fields from the ODA and the TDA be zero in the inter-region, i.e.,

$$\langle \hat{v}_\lambda\rangle_\infty \equiv \frac{1}{V_\infty}\int_{\mathscr{V}_\infty} \hat{v}_\lambda dV = 0 \tag{23}$$

here $\mathscr{V}_\infty$ is the domain of the system occupied by the inter-region and contains portions of the ω- and η-regions; so that $\mathscr{V}_\infty = \mathscr{V}_\omega + \mathscr{V}_\eta$ [12] and

$$\hat{v}_\lambda = \begin{cases} \hat{v}_\eta, & \text{in } \mathscr{V}_\eta \\ \hat{v}_\omega, & \text{in } \mathscr{V}_\omega \end{cases} \tag{24}$$

For the one-dimensional problem under consideration we can express Eq. (23) as

$$\int_{-y_\omega}^{y_0} \hat{v}_\omega dy + \int_{y_0}^{y_\eta} \hat{v}_\eta dy = 0 \tag{25a}$$

with $y = -y_\omega$ and $y = y_\eta$ locating the limits of the inter-region.

Second integral constraint:
Require that the differences of the governing equations for the velocity fields from the ODA and TDA be zero in the inter-region. This is the approach originally proposed by Ochoa-Tapia and Whitaker [12]. The result of subtracting the governing equations for the ODA and the TDA is given in Eq. (16). Therefore, this constraint requires integrating Eq. (16a) from $y = y_0$ to $y = y_\eta$ and also integrating Eq. (16b) from $y = -y_\omega$ to $y = y_0$ and adding the resulting expressions, yielding

$$\begin{aligned}
&(1 + \ln\varepsilon_\beta(y_0))\frac{d\langle v_\beta\rangle^\beta_\eta}{dy}\Big|_{y_0} - \left(1 + \ln\frac{\varepsilon_\beta(y_0)}{\varepsilon_{\beta\omega}}\right)\frac{d\langle v_\beta\rangle^\beta_\omega}{dy}\Big|_{y_0} \\
&+ \int_{-y_\omega}^{y_\eta}\left(M_\beta - \frac{d\ln\varepsilon_\beta}{dy}\frac{d}{dy}\right)\hat{v}_\lambda dy \\
&+ \left[\int_{y_0}^{y_\eta} M_\beta dy\right]\langle v_\beta\rangle^\beta_\eta\Big|_{y_0} \\
&+ \left[\int_{-y_\omega}^{y_0}\left(M_\beta + \varepsilon_{\beta\omega}K^{-1}_{\beta\omega}\right)dy\right]\langle v_\beta\rangle^\beta_\omega\Big|_{y_0} = 0
\end{aligned} \tag{25b}$$

here we have used the boundary conditions given in Eqs. (18) and (20b).

From the above, we notice that, while both integral constraints given in eqs. (25a) and (25b) arise from the same idea that the ODA should be satisfied on the average, these equations are both linearly independent and can be used to obtain the associated boundary conditions. This is shown in the following paragraphs. Indeed, other possibilities could have been proposed; for example performing weighted averages of each integrals in Eq. (25a). However, the expressions here proposed are those that, from our point of view, most clearly and satisfactorily meet the requirement for

the fields of the TDA to reproduce those of the ODA on the average. In addition, the first integral constraint, as expressed in Eq. (23), resembles the typical average constraint that bounds the fields of the closure variables in the method of volume averaging and, in this particular case, implies that the flowrates from the ODA and TDA must be the same in the inter-region.

3.2.1. First jump condition

As explained above, the complete statement of the boundary-value problem for the two-domain approach requires establishing two boundary conditions at the dividing surface. The first one can be obtained by substituting the solution of the macroscopic closure problem given by Eqs. (21) into the integral constraint in Eq. (25a); the resulting expression is

$$\left.\frac{d\langle v_\beta\rangle_\eta^\beta}{dy}\right|_{y_0} - \alpha_{\eta\omega}\frac{\alpha}{\sqrt{K_{\beta\omega}}}\left.\frac{d\langle v_\beta\rangle_\omega^\beta}{dy}\right|_{y_0} = \frac{\alpha}{\sqrt{K_{\beta\omega}}}\left(\left.\langle v_\beta\rangle_\eta^\beta\right|_{y_0} - \varepsilon_{\beta\omega}\vartheta\left.\langle v_\beta\rangle_\omega^\beta\right|_{y_0}\right) \tag{26}$$

which was conveniently written to resemble the jump condition proposed by Beavers and Joseph [17]; however, contrary to this classical boundary condition, the result in Eq. (26) is written in terms of three jump coefficients instead of one. These coefficients are defined in terms of the macroscopic closure variables according to the following definitions

$$\alpha_{\eta\omega} = \frac{\int_{y=-y_\omega}^{y=y_0} b_{\omega\omega}dy + \int_{y=y_0}^{y=y_\eta} b_{\eta\omega}dy}{\int_{y=-y_\omega}^{y=y_0} s_{\omega\eta}dy + \int_{y=y_0}^{y=y_\eta} s_{\eta\eta}dy} \tag{27a}$$

$$\frac{\alpha}{\sqrt{K_{\beta\omega}}} = -\frac{\int_{y=-y_\omega}^{y=y_0} s_{\omega\eta}dy + \int_{y=y_0}^{y=y_\eta} s_{\eta\eta}dy}{\int_{y=-y_\omega}^{y=y_0} b_{\omega\eta}dy + \int_{y=y_0}^{y=y_\eta} b_{\eta\eta}dy} \tag{27b}$$

$$\varepsilon_{\beta\omega}\vartheta = -\frac{\int_{y=-y_\omega}^{y=y_0} s_{\omega\omega}dy + \int_{y=y_0}^{y=y_\eta} s_{\eta\omega}dy}{\int_{y=-y_\omega}^{y=y_0} s_{\omega\eta}dy + \int_{y=y_0}^{y=y_\eta} s_{\eta\eta}dy} \tag{27c}$$

3.2.2. Second jump condition

To determine the second boundary condition, we substitute the solution of the macroscopic closure problems into the integral constraint given by Eq. (25b), the result can be written as

$$\left.\frac{d\langle v_\beta\rangle_\omega^\beta}{dy}\right|_{y_0} - \varpi\left.\frac{d\langle v_\beta\rangle_\eta^\beta}{dy}\right|_{y_0} = \frac{\varepsilon_{\beta\omega}\beta}{\sqrt{K_{\beta\omega}}}\left(\left.\langle v_\beta\rangle_\omega^\beta\right|_{y_0} - \beta_{\omega\eta}\left.\langle v_\beta\rangle_\eta^\beta\right|_{y_0}\right) \tag{28}$$

which, in this case, was conveniently arranged to resemble the jump condition derived by Ochoa-Tapia and Whitaker [12]. As in the previous boundary condition, the coefficients involved in Eq. (28) are defined in terms of integrals of the corresponding closure variables according to the following expressions

$$\varpi = \frac{1 + \ln\varepsilon_\beta(y_0) + \int_{-y_\omega}^{y_\eta}\left(M_\beta - \frac{d\ln\varepsilon_\beta}{dy}\frac{d}{dy}\right)f_3 dy}{D_\omega} \tag{29a}$$

$$\frac{\varepsilon_{\beta\omega}\beta}{\sqrt{K_{\beta\omega}}} = \frac{D_\beta}{D_\omega} \tag{29b}$$

$$\beta_{\omega\eta} = -\frac{\int_{y_0}^{y_\eta} M_\beta dy + \int_{-y_\omega}^{y_\eta}\left(M_\beta - \frac{d\ln\varepsilon_\beta}{dy}\frac{d}{dy}\right)f_2 dy}{D_\beta} \tag{29c}$$

where, for the sake of simplicity in presentation, we introduced

$$D_\beta = \int_{-y_\omega}^{y_0}\left(M_\beta + \varepsilon_{\beta\omega}K_{\beta\omega}^{-1}\right)dy + \int_{-y_\omega}^{y_\eta}\left(M_\beta - \frac{d\ln\varepsilon_\beta}{dy}\frac{d}{dy}\right)f_1 dy \tag{30a}$$

$$D_\omega = 1 + \ln\frac{\varepsilon_\beta(y_0)}{\varepsilon_{\beta\omega}} - \int_{-y_\omega}^{y_\eta}\left(M_\beta - \frac{d\ln\varepsilon_\beta}{dy}\frac{d}{dy}\right)f_4 dy \tag{30b}$$

In the above expressions

$$f_i = \begin{cases} f_{\eta i}, & \text{in the}\eta - \text{ region} \\ f_{\omega i}, & \text{in the}\omega - \text{ region} \end{cases}; \quad i = 1,\ldots,4 \tag{31}$$

The expressions for $f_{\eta i}$ and $f_{\omega i}$ are available in Table 1.

Hence, with the numerical solutions of the closure problems described above, one can easily determine the jump coefficients involved in Eqs. (26) and (28). This is an advance with respect to previous works in that it is not necessary to solve the ODA to determine the jump coefficients or to carry out experiments and compute them by means of best-fit approximations.

It is evident that the solution of the macroscopic closure problems requires knowledge of the dividing surface position (y_0) and the width of the zone in which the macroscopic deviations are non-zero (*i.e.*, $y \in [-y_\omega, y_\eta]$). To determine these unknowns, we used the following strategy:

1. Propose test values of y_ω and y_η.
2. Solve the macroscopic closure problems, Eq. (22), and compute the jump coefficients for several test values of y_0.
3. The position of the dividing surface is chosen as the value that satisfies the two unused boundary conditions in Eq. (18).
4. Re-calculate the jump coefficients with the corrected position of the dividing surface.
5. Return to step 1 until the values of the effective medium coefficients and the dividing surface position are independent of the width $y_\eta + y_\omega$.

We observed that using either Dirichlet, Neumann or combinations of both types of boundary conditions yielded the same results. The reason for this is that the fields of the macroscopic deviations tend to behave as horizontal lines near the boundaries of the inter-region. For simplicity we assumed that $y_\omega = y_\eta$ and noticed that fixing $y_\eta = 10r_0$ was sufficient to satisfy point 5 of the above algorithm. Using this strategy, we obtained the results presented in Table 2 for porosity values between 0.3 and 0.9. This is the porosity values range for which we have available predictions of the spatial variations of the permeability [26]. Regarding the results in Table 2, the following observations are in order

- The position of the dividing surface is, in all cases, positive and equals to $1.02r_0$.
- The jump coefficient ϑ decreases with the porosity, indicating that the difference of the velocities at the dividing surface should also decrease with porosity.
- The jump coefficients α and $\alpha_{\eta\omega}$ are increasing functions of the porosity and are of the same order of magnitude.
- The jump coefficient ϖ is practically the unity for all the cases studied, suggesting that the fluxes at the dividing surface are of the same order of magnitude.
- The jump coefficient β is negative in all cases and decreases, in absolute value, with the porosity.
- The jump coefficient $\beta_{\omega\eta}$ is practically zero, and as consequence, the stress jump is mainly caused by $\left.\langle v_\beta\rangle_\omega^\beta\right|_{y_0}$.

In this way, the two-domain approach consists of the differential equations (12), which are subjected to the boundary conditions given in Eq. (9), (26) and (28). Whereas the one-domain approach only involves one differential equation with-variable coefficients, Eq. (11), which is subject to the boundary conditions given in Eq. (9). Before comparing the predictions from these two modeling approaches, it is convenient to apply the methodology here proposed

to the conditions studied by Beavers and Joseph [17] and Ochoa-Tapia and Whitaker [12].

4. Case study I: Beavers and Joseph

These authors proposed to use Darcy's law within the entire domain occupied by the porous medium. This implies that the velocity $\langle v_\beta\rangle_\omega^\beta$ is a constant and equals $\langle v_\beta\rangle_{\omega,\infty}^\beta$. This can be corroborated from Eq. (12b) by simply assuming that $\langle v_\beta\rangle_\omega^\beta$ is a constant, which allows reducing this expression to the algebraic equation

$$0 = -\varepsilon_{\beta\omega}K_{\beta\omega}^{-1}\left(\langle v_\beta\rangle_\omega^\beta - \langle v_\beta\rangle_{\omega,\infty}^\beta\right), \quad \forall y \in (-L_\omega, y_0) \tag{32}$$

while Eq. (12a) is still applicable in the fluid phase. Under the assumption of constant velocity in the porous medium, the macroscopic closure problem takes the following form,

$$0 = L(\hat{v}_\eta) - \underbrace{\varepsilon_\beta^{-1}\frac{d\varepsilon_\beta}{dy}\frac{d\langle v_\beta\rangle_\eta^\beta}{dy}\Big|_{y_0}}_{\text{source}} + \underbrace{M_\beta\langle v_\beta\rangle_\eta^\beta\big|_{y_0}}_{\text{source}} \quad \forall y \in \left(y_0, y_\eta\right) \tag{33a}$$

$$0 = L(\hat{v}_\omega) + \underbrace{\left(M_\beta + \varepsilon_{\beta\omega}K_{\beta\omega}^{-1}\right)\langle v_\beta\rangle_\omega^\beta\big|_{y_0}}_{\text{source}} \quad \forall y \in (-y_\omega, y_0) \tag{33b}$$

$$\text{at } y = y_\eta \quad \hat{v}_\eta = 0; \quad \frac{d\hat{v}_\eta}{dy} = 0 \tag{33c}$$

$$\text{at } y = -y_\omega, \quad \hat{v}_\omega = 0; \quad \frac{d\hat{v}_\omega}{dy} = 0 \tag{33d}$$

$$\text{at } y_0, \quad \hat{v}_\omega + \underbrace{\langle v_\beta\rangle_\omega^\beta\big|_{y_0}}_{\text{source}} = \hat{v}_\eta + \underbrace{\langle v_\beta\rangle_\eta^\beta\big|_{y_0}}_{\text{source}} \tag{33e}$$

$$\text{at } y_0, \quad \frac{d\hat{v}_\omega}{dy} = \frac{d\hat{v}_\eta}{dy} + \underbrace{\frac{d\langle v_\beta\rangle_\eta^\beta}{dy}\Big|_{y_0}}_{\text{source}} \tag{33f}$$

Notice that there are only three sources in this closure problem, consequently the solution given in Eq. (21) can be reduced to

$$\hat{v}_\omega = s_{\omega\eta}\langle v_\beta\rangle_\eta^\beta\big|_{y_0} + s_{\omega\omega}\langle v_\beta\rangle_\omega^\beta\big|_{y_0} + b_{\omega\eta}\frac{d\langle v_\beta\rangle_\eta^\beta}{dy}\Big|_{y_0} \tag{34a}$$

$$\hat{v}_\eta = s_{\eta\eta}\langle v_\beta\rangle_\eta^\beta\big|_{y_0} + s_{\eta\omega}\langle v_\beta\rangle_\omega^\beta\big|_{y_0} + b_{\eta\eta}\frac{d\langle v_\beta\rangle_\eta^\beta}{dy}\Big|_{y_0} \tag{34b}$$

The six closure variables involved in the above expressions satisfy the general closure problem given in Eq. (22) and the corresponding entries are available in Table 3. This feature is convenient in the development of the numerical routine to solve the closure problems and compute the corresponding jump coefficients.

Since, in this case, the TDA involves only one second-order differential equation (Eq. 12a), the statement of the boundary problem requires solely two boundary conditions. One of them corresponds to the boundary $y = L_\eta$ and is given by Eq. (9b). The remaining boundary condition applies at $y = y_0$ and results from the substitution of Eq. (34) into the average constraint given in Eq. (25a) and can be expressed as

$$\frac{d\langle v_\beta\rangle_\eta^\beta}{dy}\Big|_{y_0} = \frac{\alpha}{\sqrt{K_{\beta\omega}}}\left(\langle v_\beta\rangle_\eta^\beta\big|_{y_0} - \varepsilon_{\beta\omega}\vartheta\langle v_\beta\rangle_\omega^\beta\big|_{y_0}\right) \tag{35}$$

Table 3
Dependent variables and sources for the closure problems resulting from adopting the assumptions by Beavers and Joseph (BJ) [17].

Source	i	$f_{\lambda i}$		$\Psi_{\lambda i}$		BJ	
		$\lambda=\eta$	$\lambda=\omega$	$\lambda=\eta$	$\lambda=\omega$	ψ_i	Γ_i
$\langle v_\beta\rangle_\omega^\beta\big\|_{y_0}$	1	$s_{\eta\omega}$	$s_{\omega\omega}$	0	$-(M_\beta + \varepsilon_{\beta\omega}K_{\beta\omega}^{-1})$	−1	0
$\langle v_\beta\rangle_\eta^\beta\big\|_{y_0}$	2	$s_{\eta\eta}$	$s_{\omega\eta}$	$-M_\beta$	0	1	0
$\frac{d\langle v_\beta\rangle_\eta^\beta}{dy}\big\|_{y_0}$	3	$b_{\eta\eta}$	$b_{\omega\eta}$	$\frac{d\ln\varepsilon_\beta}{dy}$	0	0	1

Here the jump coefficients α and ϑ are defined by eqs. (27b) and (27c), respectively. Notice that the classical condition proposed by Beavers and Joseph [17] is exactly recovered if $\vartheta = 1$. Using the solution algorithm presented above, we computed the jump coefficients involved in Eq. (35) as well as the position of the dividing surface. The results for several porosity values are given in Table 4. In this case we observe the following:

- The position of the dividing surface is, in all cases, negative and it tends to the value $-r_0$. This result is to be expected since this model does not involve Brinkman's contribution, which is relevant near the porous medium-fluid boundary.
- The jump coefficient ϑ decreases with the porosity and reaches values near zero. However, it can be demonstrated that, in the limit as $\varepsilon_{\beta\omega} \to 1$, $\vartheta \to 1$. As pointed out above, the original jump condition by Beavers and Joseph requires that $\vartheta = 1$ for all porosity values. Since this is not the case, the predictions from this model should not be confused as those from the Beavers and Joseph model. To avoid any confusion, we refer to this TDA version as the one resulting from adopting the assumptions by Beavers and Joseph (*i.e.*, neglecting Brinkman's correction).
- The jump coefficient α is, in all cases, negative and increases, in absolute value, with the porosity. However, the ratio $\alpha/\sqrt{K_{\beta\omega}}$ decreases, in absolute value, with the porosity.

In summary, in this case, the TDA consists of eqs. (12a) and (32), together with the boundary conditions given in eqs. (9b) and (35). The analytical solution of this model, together with the comparison with the other upscaling approaches will be presented in subsequent paragraphs.

5. Case study II: Ochoa-Tapia and Whitaker

In their work, Ochoa-Tapia and Whitaker [12], utilized Eq. (12) as the TDA; the key difference between their approach and the one presented above is that these authors imposed the continuity of the surface averaged velocities at the dividing surface. In terms of intrinsic averaged quantities, this assumption can be written as

$$\text{at } y = y_0, \quad \varepsilon_{\beta\omega}\langle v_\beta\rangle_\omega^\beta\big|_{y_0} = \langle v_\beta\rangle_\eta^\beta\big|_{y_0} \tag{36}$$

Table 4
Position of the dividing surface and jump coefficients involved in the TDA adopting the assumptions by Beavers and Joseph [17] for several porosity values.

$\varepsilon_{\beta\omega}$	y_0/r_0	ϑ	α
0.3	-0.695	5.09×10^{-2}	-35.1
0.4	-0.981	1.24×10^{-4}	-50.6
0.5	-0.823	5.76×10^{-3}	-52.8
0.6	-0.936	4.07×10^{-4}	-73.0
0.7	-0.996	1.25×10^{-5}	-97.1
0.8	-0.996	1.47×10^{-5}	-101.9
0.9	-1.010	1.08×10^{-5}	-183.4

As consequence, the macroscopic closure problem is now

$$0 = L(\hat{v}_\eta) - \underbrace{\varepsilon_\beta^{-1}\frac{d\varepsilon_\beta}{dy}\frac{d\langle v_\beta\rangle_\eta^\beta}{dy}\Big|_{y_0}}_{\text{source}} + \underbrace{M_\beta\varepsilon_{\beta\omega}\langle v_\beta\rangle_\omega^\beta\Big|_{y_0}}_{\text{source}} \quad \forall y\in\left(y_0,y_\eta\right) \tag{37a}$$

$$0 = L(\hat{v}_\omega) - \underbrace{\varepsilon_\beta^{-1}\frac{d\varepsilon_\beta}{dy}\frac{d\langle v_\beta\rangle_\omega^\beta}{dy}\Big|_{y_0}}_{\text{source}} + \underbrace{\left(M_\beta+\varepsilon_{\beta\omega}K_{\beta\omega}^{-1}\right)\langle v_\beta\rangle_\omega^\beta\Big|_{y_0}}_{\text{source}} \quad \forall y\in(-y_\omega,y_0) \tag{37b}$$

$$\text{at } y=y_\eta \quad \hat{v}_\eta = 0; \quad \frac{d\hat{v}_\eta}{dy} = 0 \tag{37c}$$

$$\text{at } y=-y_\omega, \quad \hat{v}_\omega = 0; \quad \frac{d\hat{v}_\omega}{dy} = 0 \tag{37d}$$

$$\text{at } y_0, \quad \hat{v}_\omega = \hat{v}_\eta + (\varepsilon_{\beta\omega}-1)\underbrace{\langle v_\beta\rangle_\omega^\beta\Big|_{y_0}}_{\text{source}} \tag{37e}$$

$$\text{at } y_0, \quad \frac{d\hat{v}_\omega}{dy} + \underbrace{\frac{d\langle v_\beta\rangle_\omega^\beta}{dy}\Big|_{y_0}}_{\text{source}} = \frac{d\hat{v}_\eta}{dy} + \underbrace{\frac{d\langle v_\beta\rangle_\eta^\beta}{dy}\Big|_{y_0}}_{\text{source}} \tag{37f}$$

As in the previous case, there are three sources for the closure problem, which are not the same as those resulting from imposing the assumptions made by BJ. The macroscopic closure problem solution is thus

$$\hat{v}_\omega = s_{\omega\omega}\langle v_\beta\rangle_\omega^\beta\Big|_{y_0} + b_{\omega\eta}\frac{d\langle v_\beta\rangle_\eta^\beta}{dy}\Big|_{y_0} + b_{\omega\omega}\frac{d\langle v_\beta\rangle_\omega^\beta}{dy}\Big|_{y_0} \tag{38a}$$

$$\hat{v}_\eta = s_{\eta\omega}\langle v_\beta\rangle_\omega^\beta\Big|_{y_0} + b_{\eta\eta}\frac{d\langle v_\beta\rangle_\eta^\beta}{dy}\Big|_{y_0} + b_{\eta\omega}\frac{d\langle v_\beta\rangle_\omega^\beta}{dy}\Big|_{y_0} \tag{38b}$$

As before, the closure variables involved in the above solutions satisfy the general closure problem given by Eq. (22); the corresponding entries are provided in Table 5.

As in our first version of the TDA, in this case, there are two differential equations that must be coupled at the dividing surface by appropriate boundary conditions. The first one is the assumption given in Eq. (36); the second one results from substituting the macroscopic closure problem solutions (Eq. (38)) into the integral constraint given by Eq. (25b). The resulting boundary condition is

$$\frac{d\langle v_\beta\rangle_\omega^\beta}{dy}\Big|_{y_0} - \varpi\frac{d\langle v_\beta\rangle_\eta^\beta}{dy}\Big|_{y_0} = \frac{\varepsilon_{\beta\omega}\beta_{OTW}}{\sqrt{K_{\beta\omega}}}\langle v_\beta\rangle_\omega^\beta\Big|_{y_0} \tag{39}$$

where, in order to resemble the boundary condition by Ochoa-Tapia and Whitaker [12], we defined

$$\beta_{OTW} = \beta(1-\beta_{\omega\eta}\varepsilon_{\beta\omega}) \tag{40}$$

The definitions of ϖ, β and $\beta_{\omega\eta}$ in terms of the corresponding closure variables are given in Eq. (29). As in the previous case, there are only two jump coefficients to be determined from the closure problem solutions. Using the solution scheme outlined in previous sections we obtained the results displayed in Table 6. Regarding these results, we have the following comments:

- The dividing surface position is positive and decreases with the porosity. As in the previous cases $y_0 = \mathbf{O}(r_0)$.
- The jump coefficient $\varpi = 1$ for all the cases here studied, thus suggesting that the derivatives of the velocity at y_0 are of the same order.
- The values of β_{OTW} are negative and $\mathbf{O}(1)$. Although not shown in Table 6, the values of $\beta_{\omega\eta}$ are $\mathbf{O}(10^{-2})$, thus from Eq. (40), we have that $\beta \approx \beta_{OTW}$.

In addition, it is worth adding that the values and sign of the jump coefficient β_{OTW} are highly sensitive to the dividing surface position. As a matter of fact, if one arbitrarily fixes $y_0 = 0$, it results that $\beta_{OTW} > 0$, which is consistent with previous studies (cf. [23]).

Summing up, in this case, the TDA consists of Eq. (12) subject to the boundary conditions given in Eq. (9), (36) and (39). In the following section we will compare the three versions of the TDA here proposed with those resulting from the ODA.

6. Models evaluation

In the previous sections we derived the boundary-value problems describing the one and two domain approaches for the system under consideration. In this section we will evaluate the velocity profiles resulting from each modeling approach. To this end, we first note that, due to the non-trivial position dependence of the effective medium coefficients (porosity and permeability) involved in the ODA (see Eq. 11), it has not been possible to obtain an analytical solution. For this reason, we used finite differences schemes, with a sufficiently fine mesh, to solve the boundary-value problem given by Eqs. (11) and (9). Standard tests of convergence and uniqueness were performed in order to guarantee the reliability of the numerical solution.

For the three versions of the TDA, it is possible to obtain analytical solutions; for the BJ problem, the solution for the η-region is

$$\frac{\langle v_\beta\rangle_\eta^\beta}{\langle v_\beta\rangle_{\omega,\infty}^\beta} = L_\eta\left(1-\frac{y}{L_\eta}\right)\left[\frac{\varepsilon_{\beta\omega}}{2K_{\beta\omega}}L_\eta\left(1+\frac{y}{L_\eta}\right) - c_{BJ}\right] \tag{41}$$

with c_{BJ} being

$$c_{BJ} = \varepsilon_{\beta\omega}\frac{\frac{L_\eta^2}{2K_{\beta\omega}}\left(1-\frac{y_0^2}{L_\eta^2}\right) + \frac{\sqrt{K_{\beta\omega}}}{\alpha}\frac{y_0}{K_{\beta\omega}} - \vartheta}{L_\eta\left(1-\frac{y_0}{L_\eta}\right) + \frac{\sqrt{K_{\beta\omega}}}{\alpha}} \tag{42}$$

whereas in the porous medium region $\langle v_\beta\rangle_\omega^\beta = \langle v_\beta\rangle_{\omega,\infty}^\beta$.

Table 5
Dependent variables and sources for the closure problems involved in the TDA adopting the assumptions by Ochoa-Tapia and Whitaker (OTW) [12].

Source	i	$f_{\lambda i}$		$\Psi_{\lambda i}$		OTW	
		$\lambda=\eta$	$\lambda=\omega$	$\lambda=\eta$	$\lambda=\omega$	ψ_i	Γ_i
$\langle v_\beta\rangle_\omega^\beta\big\|_{y_0}$	1	$s_{\eta\omega}$	$s_{\omega\omega}$	$-M_\beta\varepsilon_{\beta\omega}$	$-(M_\beta+\varepsilon_{\beta\omega}K_{\beta\omega}^{-1})$	$\varepsilon_{\beta\omega}-1$	0
$\frac{d\langle v_\beta\rangle_\eta^\beta}{dy}\big\|_{y_0}$	3	$b_{\eta\eta}$	$b_{\omega\eta}$	$\frac{d\ln\varepsilon_\beta}{dy}$	0	0	1
$\frac{d\langle v_\beta\rangle_\omega^\beta}{dy}\big\|_{y_0}$	4	$b_{\eta\omega}$	$b_{\omega\omega}$	0	$\frac{d\ln\varepsilon_\beta}{dy}$	0	−1

Table 6
Position of the dividing surface and jump coefficients involved in the TDA adopting the assumptions by Ochoa-Tapia and Whitaker [12] for several porosity values.

$\varepsilon_{\beta\omega}$	y_0/r_0	ϖ	β_{OTW}
0.3	0.853	0.99	−0.498
0.4	0.853	0.99	−0.528
0.5	0.833	1.00	−0.464
0.6	0.828	1.00	−0.425
0.7	0.808	1.00	−0.393
0.8	0.768	1.00	−0.401
0.9	0.727	1.00	−0.362

For the TDA derived in this work, the solution of the corresponding boundary-value problem is

$$\frac{\langle v_\beta\rangle_\omega^\beta}{\langle v_\beta\rangle_{\omega,\infty}^\beta} = c_\omega\left[\exp\left(\sqrt{\frac{\varepsilon_{\beta\omega}}{K_{\beta\omega}}}y\right) - \exp\left(-\sqrt{\frac{\varepsilon_{\beta\omega}}{K_{\beta\omega}}}(y+2L_\omega)\right)\right] + 1 \tag{43a}$$

$$\frac{\langle v_\beta\rangle_\eta^\beta}{\langle v_\beta\rangle_{\omega,\infty}^\beta} = L_\eta\left(1-\frac{y}{L_\eta}\right)\left[\frac{\varepsilon_{\beta\omega}}{2K_{\beta\omega}}L_\eta\left(1+\frac{y}{L_\eta}\right) - c_\eta\right] \tag{43b}$$

here the constants c_ω and c_η are

$$c_\eta = -\frac{A_{22}}{A_{21}} - \left(A_{12} - \frac{A_{11}A_{22}}{A_{21}}\right)\frac{(1-\beta\sqrt{\varepsilon_{\beta\omega}})\sqrt{\frac{\varepsilon_{\beta\omega}}{K_{\beta\omega}}} + (1+\beta\sqrt{\varepsilon_{\beta\omega}})\sqrt{\frac{\varepsilon_{\beta\omega}}{K_{\beta\omega}}}E_2}{B_- + B_+E_2} \tag{44a}$$

$$c_\omega = \frac{A_{12}A_{21} - A_{11}A_{22}}{B_- + B_+E_2}\exp\left(-\sqrt{\frac{\varepsilon_{\beta\omega}}{K_{\beta\omega}}}y_0\right) \tag{44b}$$

As a matter of convenience, we defined the following parameters in the above expressions

$$A_{11} = -L_\eta\left(1-\frac{y_0}{L_\eta}\right) - \frac{\sqrt{K_{\beta\omega}}}{\alpha} \tag{45a}$$

$$A_{12} = \varepsilon_{\beta\omega}\left(\frac{L_\eta^2}{2K_{\beta\omega}}\left(1-\frac{y_0^2}{L_\eta^2}\right) - \vartheta + \frac{y_0}{\alpha\sqrt{K_{\beta\omega}}}\right) \tag{45b}$$

$$A_{22} = \frac{\varepsilon_{\beta\omega}\varpi}{K_{\beta\omega}}y_0 - \frac{\varepsilon_{\beta\omega}\beta}{\sqrt{K_{\beta\omega}}}\left[1 - \frac{\beta_{\omega\eta}\varepsilon_{\beta\omega}}{2K_{\beta\omega}}L_\eta^2\left(1-\frac{y_0^2}{L_\eta^2}\right)\right] \tag{45c}$$

$$A_{21} = -\left[\varpi + \frac{\varepsilon_{\beta\omega}\beta}{\sqrt{K_{\beta\omega}}}\beta_{\omega\eta}L_\eta\left(1-\frac{y_0}{L_\eta}\right)\right] \tag{45d}$$

$$f_\pm = A_{11}(1\pm\beta\sqrt{\varepsilon_{\beta\omega}})\sqrt{\frac{\varepsilon_{\beta\omega}}{K_{\beta\omega}}} \mp A_{21}\left(\varepsilon_{\beta\omega}\vartheta \pm \alpha_{\eta\omega}\sqrt{\frac{\varepsilon_{\beta\omega}}{K_{\beta\omega}}}\right) \tag{45e}$$

Finally, the solution of the TDA, under the velocity continuity assumption, is still the one given by Eqs. (43)–(45) fixing $\vartheta = 1$, $\sqrt{K_{\beta\omega}}\alpha^{-1} = 0$ and $\alpha_{\eta\omega} = 0$. In the following, we will present the predictions for the superficial averaged velocity in the following dimensionless form

$$U = \frac{\langle v_\beta\rangle}{\max(\langle v_\beta\rangle)};\quad U_\lambda = \frac{\langle v_\beta\rangle_\lambda}{\max(\langle v_\beta\rangle)}, \lambda = \omega,\eta \tag{46}$$

The first of these corresponds to the ODA and the second one to the TDA. In Fig. 3 we show an example of the velocity profiles resulting from the ODA and TDA taking $\varepsilon_{\beta\omega} = 0.7$ and $L_\eta = L_\omega = 1000r_0$. From the plots in Figs. 3(a) and (d) we barely observe any difference between the velocity profiles predicted from either approach. To gain a better insight, we show in Figs. 3(b) and (e) a zoom near the maximum velocity in the free fluid region. From these results we observe that the TDA involving two jump conditions proposed in this work is the closest to the ODA, followed by the one resulting from adopting the assumptions made by Ochoa-Tapia and Whitaker [12]. Finally, the TDA resulting from adopting the assumptions made by Beavers and Joseph [17] exhibits the largest deviations from the ODA. These observations are the result of the velocity and stress values predicted at the dividing surface (see Fig. 3(f)). Notice that the velocity profiles from this work and those from accepting the assumptions by Ochoa-Tapia and Whitaker are close to each other and appear to be quite similar to those from the ODA (Fig. 3(c)). This can be attributed to the proximity in the values of the dividing surface position (see Tables 2 and 6). Furthermore, from Table 4 we observe that the dividing surface position for the TDA adopting the assumptions proposed by Beavers and Joseph lies in the porous medium region and this causes the velocity profiles to be noticeably far from the rest. This situation can surely be reversed if one arbitrarily fixes the dividing surface position to be on the side of the fluid in this model. Finally, it should be stressed that the velocity profiles from the TDA involving the assumptions made by BJ are discontinuous at $y = y_0$, however this discontinuity is not appreciable at the level of resolution used in Fig. 3(f).

To gain a more quantitative insight about the predictive capabilities of the three alternatives of the TDA to reproduce the maximum velocity in the free fluid region, we show in Table 7 the relative error percent

$$\text{Error}\% = \frac{|U-U_\eta|}{U}\times 100\% \tag{47}$$

of the three modeling alternatives as function of the porous medium porosity. We observe that this percent is $\mathbf{O}(10^{-4})$ for the TDA proposed in this work and it increases in two orders of magnitude if one adopts the assumption of continuity of the superficial averaged velocity at the dividing surface as proposed by Ochoa-Tapia and Whitaker [12]. Finally, if one neglects the Brinkman's correction in the TDA, as originally assumed by Beavers and Joseph [17], the relative error percent for predicting the maximum velocity is $\mathbf{O}(10^{-1})$. This implies that the prediction of the velocity and stress at the dividing surface does not have a drastic effect over the predictions of the maximum velocities for the three alternatives of the TDA here studied.

At this point it is worth recalling that the purpose of the jump conditions is to replace the zone of changes (*i.e.*, the inter-region) involved in the ODA by a dividing surface as sketched in Fig. 2. With this in mind, to conclude this section, we compute the TDA predictions for the slip velocity and evaluate if they satisfy, on the average, the velocity profiles from the ODA. To this end, we define the ODA velocity averaged over the inter-region as

$$\langle U\rangle_0 = \frac{1}{2r_0}\int_{y=-r_0}^{y=+r_0} U dy \tag{48}$$

In Table 8 we show the values of $\langle U\rangle_0$ and the slip velocities from the three versions of the TDA for several porosity values. For the TDA proposed here, $\langle U\rangle_0$ is found to lie between the two slip velocities $U_\omega|_{y_0}$ and $U_\eta|_{y_0}$. This is to be expected since the purpose of the jump conditions is to capture, on the average, the information arising from the ODA. In this way, it is also to be expected that the slip velocity $U_\omega|_{y_0}$ ($= U_\eta|_{y_0}$) resulting from the TDA with the assumption proposed by Ochoa-Tapia and Whitaker [12] is of the same order of magnitude as $\langle U\rangle_0$ for all the cases here studied. Finally, the predictions of the slip velocities from the TDA adopting the assumptions

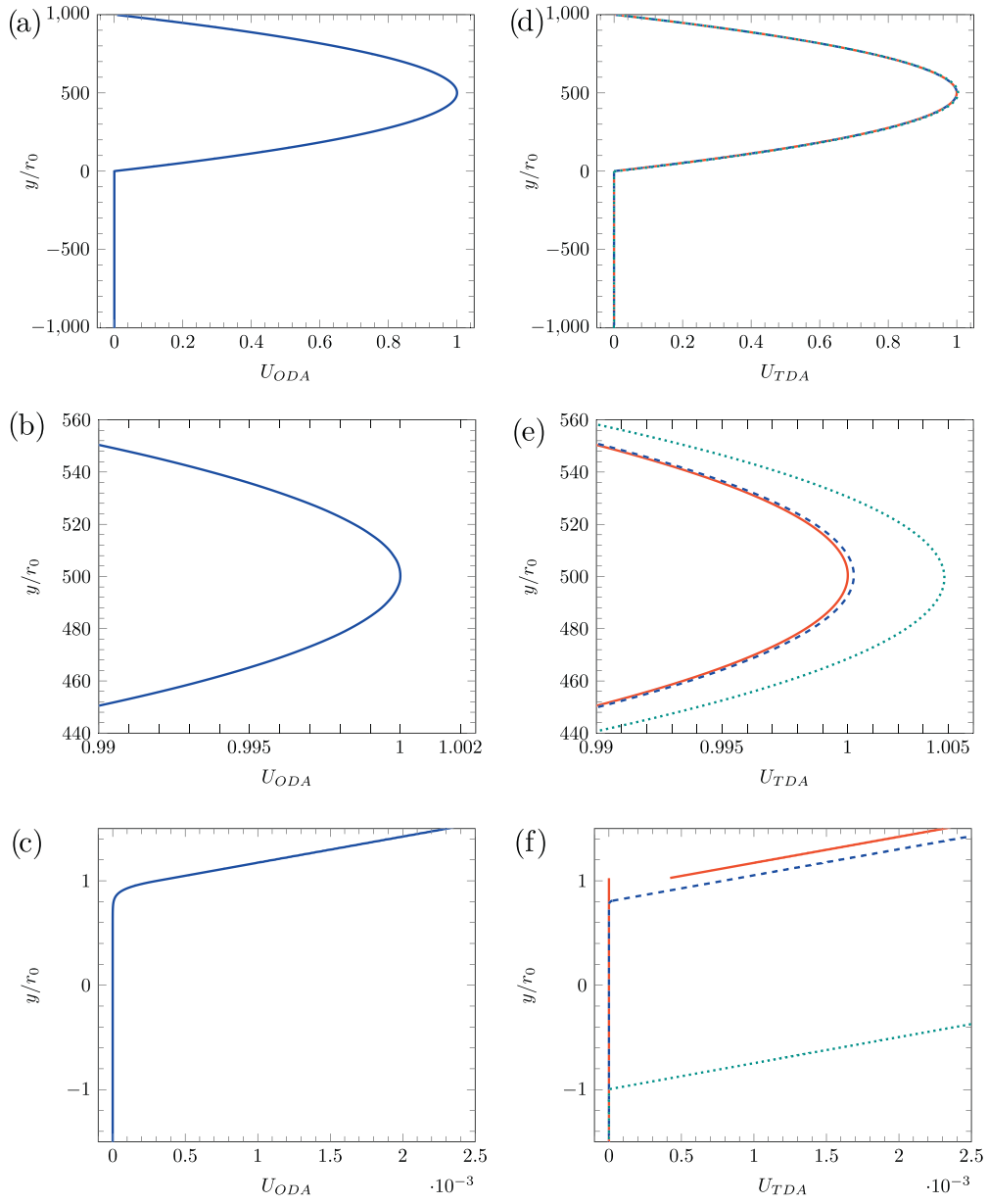

Fig. 3. Macroscopic velocity profiles obtained using the ODA (a, b and c) and the TDA (d, e and f) taking $\varepsilon_{\beta\omega} = 0.7$. For the TDA: (—) This work, (- - -) based on the assumptions by Ochoa-Tapia and Whitaker [12] and (···) based on the assumptions by Beavers and Joseph [17].

Table 7
Relative error percent of the TDA with respect to the ODA for predicting the maximum velocity at several porosities.

$\varepsilon_{\beta\omega}$	This work	OTW	BJ
0.3	2.46×10^{-4}	1.82×10^{-2}	0.328
0.4	3.04×10^{-4}	1.86×10^{-2}	0.386
0.5	3.66×10^{-4}	2.06×10^{-2}	0.352
0.6	3.06×10^{-4}	2.09×10^{-2}	0.374
0.7	2.56×10^{-4}	2.41×10^{-2}	0.385
0.8	4.32×10^{-4}	2.67×10^{-2}	0.378
0.9	5.65×10^{-4}	2.91×10^{-2}	0.375

proposed by Beavers and Joseph [17] do not comprehend the value of $\langle U \rangle_0$ from the ODA. This result is attributed to the fact that the dividing surface position for the TDA is considerably far from the one predicted by the other versions of the TDA (see Tables 2, 4 and 6).

7. Discussion and conclusions

In this work we deduced a set of boundary conditions that complete the statement of the two-domain approach for one-dimensional momentum transport in a system composed of a porous medium and a fluid under a constant pressure gradient. These boundary conditions involve a jump in both the velocity and the viscous stress and are expressed in terms of jump coefficients. This feature distinguishes our work from those by Ochoa-Tapia and Whitaker [12] and by Beavers and Joseph [17]. In the first case, continuity of the velocity was imposed and a jump condition for the stress was derived in terms of only one jump coefficient. In the second case, Beavers and Joseph extended the use of Darcy's law to the entire porous medium, thus requiring to specify one jump coefficient for the discontinuity of the velocity at the porous medium surface. In our formulation, there are two boundary conditions and six jump coefficients to be determined. However, from our computations, we observed that $\varpi \approx 1$ and $\beta_{\omega\eta} \to 0$, thus

Table 8
Predictions of the slip velocities from the three versions of the TDA and the ODA velocity averaged over the inter-region for several porosity values.

$\varepsilon_{\beta\omega}$	ODA	This work		OTW	BJ	
	$\langle U\rangle_0$	$U_\omega\|_{y_0}$	$U_\eta\|_{y_0}$	$U_\omega\|_{y_0}$	$U_\omega\|_{y_0}$	$U_\eta\|_{y_0}$
0.3	3.2×10^{-6}	4.9×10^{-9}	3.1×10^{-4}	3.5×10^{-6}	3.3×10^{-11}	1.2×10^{-7}
0.4	3.3×10^{-6}	9.1×10^{-9}	3.3×10^{-4}	5.2×10^{-6}	6.0×10^{-11}	2.1×10^{-7}
0.5	4.9×10^{-6}	15.5×10^{-9}	3.7×10^{-4}	8.3×10^{-6}	1.2×10^{-10}	3.4×10^{-7}
0.6	6.0×10^{-6}	27.4×10^{-9}	3.9×10^{-4}	13.5×10^{-6}	2.7×10^{-10}	4.5×10^{-7}
0.7	8.0×10^{-6}	47.3×10^{-9}	4.2×10^{-4}	21.8×10^{-6}	6.0×10^{-10}	5.4×10^{-7}
0.8	15.2×10^{-6}	75.1×10^{-9}	5.4×10^{-4}	34.4×10^{-6}	1.4×10^{-9}	6.9×10^{-7}
0.9	25.9×10^{-6}	97.3×10^{-9}	6.8×10^{-4}	56.1×10^{-6}	3.2×10^{-9}	8.0×10^{-7}

reducing the number of jump coefficients to four. Interestingly, under these conditions, the jump condition given by Eq. (28) takes the form of the one originally proposed by Ochoa-Tapia and Whitaker [12].

A salient feature of the methodology here proposed is that all the jump coefficients involved can be computed from the solution of a macroscopic closure problem that accounts for the deviations of the TDA with respect to the ODA. Furthermore, the position of the dividing surface where the jump conditions are applied is also predicted from the closure process. In a previous work [23] we were able to compute the values of the jump coefficient involved in the jump condition proposed by Ochoa-Tapia and Whitaker. However this approach had the drawback that it required the solution of the ODA and TDA in order to compute the excess properties. It also did not provide an insight about the dividing surface position, which has been found to be determinant in the predictive capabilities of the models. It is worth emphasizing that the macroscopic closure problem solution, and hence the computations of the jump coefficients, only requires accounting for the spatial variations of the porosity and permeability but not of the fields of the ODA and TDA. For this reason, future works will be devoted to the prediction of the spatial variations of effective medium coefficients in the transitions zone that separates homogeneous media.

As shown above, the derivation of the two boundary conditions results from imposing two integral equations associated to the macroscopic deviations (see Eqs. 25a and 25b) that require the ODA to be satisfied on the average as originally proposed by Ochoa-Tapia and Whitaker [12]. The expression given by Eq. (25a) can be regarded as a constraint that bounds the fields of the macroscopic deviations as usually imposed in the microscopic closure problems involved in the method of volume averaging [7]. The second constraint, expressed in Eq. (25b) follows from the original proposal made by Ochoa-Tapia and Whitaker consisting in subtracting the integral versions of the TDA to the integral version of the ODA. This expression is analogous to the solvability condition that is usually associated to Laplace's equation [27].

The approach for deriving boundary conditions was applied to complete the TDA formulation under the assumptions proposed by Ochoa-Tapia and Whitaker [12] and those by Beavers and Joseph [17]. In each application the result was a boundary condition expressed in terms of two jump coefficients, which were predicted from the closure problem solution together with the position of the dividing surface. On the one hand, since Beavers and Joseph did not consider Brinkman's correction in the porous medium, this model was unable to capture the essential information taking place in the inter-region of the ODA as shown in Table 8. On the other hand, the TDA derived here and the one corresponding to the assumptions made by Ochoa-Tapia and Whitaker predicted that the dividing surface should be located in the fluid region and this showed a stronger agreement with the ODA.

It should be stressed that a point-by-point comparison between the one and two-domain approaches near the boundary of the two regions is not possible because the ODA involves an inter-region, whereas in the TDA this zone is replaced by a dividing surface as sketched in Fig. 2. For this reason, we did not merge the plots in Figs. 3(c)–(f). However, since there is a disparity of characteristic lengths between the homogeneous regions and the inter-region, it is indeed possible to compare the predictions of the ODA and the TDA in the homogeneous regions. In this respect we found that either version of the TDA reproduces the ODA with an error percent ranging between 10^{-4} (this work) and 10^{-1} (based on the assumptions by Beavers and Joseph). Indeed, for cases in which the length-scale constraint $r_0 \ll L$ is not met, the use of the the effective medium equations based on the method of volume averaging is not guaranteed and thus the error increases drastically.

The results provided in this work, show that the proposed methodology for the derivation of jump conditions and the computation of the associated coefficients can certainly be extended to other transport situations such as the study of heat and mass transfer between homogeneous regions. These and other applications will be studied in future works.

Acknowledgments

This work was benefited from Fondo Sectorial de Investigación para la educación from CONACyT (Project number: 12511908; Arrangement number: 112087). FVP wants to thank prof. Stephen Whitaker's question posed in the year 2007 asking about the derivation of a second boundary condition. We hope that this paper provides a reasonable response.

References

[1] Bear J, Cheng A. Modeling groundwater flow and contaminant transport. Springer; 2010. http://dx.doi.org/10.1007/978-1-4020-6682-5.
[2] Séro-Guillaume O, Margerit J. Modelling forest fires. Part i: a complete set of equations derived by extended irreversible thermodynamics. Int J Heat Mass Transfer 2002;45:1705–22. http://dx.doi.org/10.1016/S0017-9310(01)00248-4.
[3] Lowe R, Shavit U, Falter J, Koseff J, Monismith S. Modeling flow in coral communities with and without waves: a synthesis of porous media and canopy flow approaches. Limnol Oceanogr 2008;53:2668–80. http://dx.doi.org/10.4319/lo.2008.53.6.2668.
[4] Yu P. Numerical simulation on oxygen transfer in a porous scaffold for animal cell culture. Int J Heat Mass Transfer 2012;55:4043–52. http://dx.doi.org/10.1016/j.ijheatmasstransfer.2012.03.046.
[5] Liu F, Cheng B, Wang L. Experimental and numerical estimation of slip coefficient in a partially porous cavity. Exp Therm Fluid Sci 2013;44:431–8. http://dx.doi.org/10.1016/j.expthermflusci.2012.08.004.
[6] Nabovati A, Amon C. Hydrodynamic boundary condition at open-porous interface: a pore-level lattice boltzmann study. Exp Therm Fluid Sci 2013;96:83–94. http://dx.doi.org/10.1007/s11242-012-0074-1.
[7] Whitaker S. The method of volume averaging. Kluwer Academic Publishers; 1999.
[8] Wood B, Valdés-Parada F. Volume averaging: local and nonlocal closures using a Green's function approach. Adv Water Resour 2013;51:139–67. http://dx.doi.org/10.1016/j.advwatres.2012.06.008.
[9] Whitaker S. Flow in porous media I: a theoretical derivation of Darcy's law. Transp Porous Media 1986;1:3–35. http://dx.doi.org/10.1007/BF01036523.

[10] Whitaker S. The Forchheimer equation: a theoretical derivation of Darcy's law. Transp Porous Media 1996;25:27–61. http://dx.doi.org/10.1007/BF00141261.
[11] Goyeau B, Lhuillier D, Gobin D, Velarde MG. Momentum transport at a fluid-porous interface. Int J Heat Mass Transfer 2003;46:4071–81. http://dx.doi.org/10.1016/S0017-9310(03)00241-2.
[12] Ochoa-Tapia J, Whitaker S. Momentum transfer at the boundary between a porous medium and a homogeneous fluid-I: theoretical development. Int J Heat Mass Transfer 1995;38:2635–46. http://dx.doi.org/10.1016/0017-9310(94)00346-W.
[13] Valdés-Parada F, Goyeau B, Ochoa-Tapia J. Jump momentum boundary condition at a fluid-porous dividing surface: derivation of the closure problem. Chem Eng Sci 2007;62:4025–39. http://dx.doi.org/10.1016/j.ces.2007.04.042.
[14] Chandesris M, Jamet D. Jump conditions and surface-excess quantities at a fluid/porous interface: a multi-scale approach. Transp Porous Media 2009;78:403–18. http://dx.doi.org/10.1007/s11242-008-9302-0.
[15] Chandesris M, Jamet D. Boundary conditions at a fluid-porous interface: an a priori estimation of the stress jump coefficients. Int J Heat Mass Transfer 2007;50:3422–36. http://dx.doi.org/10.1016/j.ijheatmasstransfer.2007.01.053.
[16] Duman T, Shavit U. An apparent interface location as a tool to solve the porous interface flow problem. Transp Porous Media 2009;78:509–24. http://dx.doi.org/10.1007/s11242-008-9286-9.
[17] Beavers G, Joseph D. Boundary conditions at a naturally permeable wall. J Fluid Mech 1967;30:197–207. http://dx.doi.org/10.1017/S0022112067001375.
[18] Neale G, Nader W. Practical significance of Brinkman's extension of Darcy's law: coupled parallel flow within a channel and a bounding porous medium. Can J Chem Eng 1974;52:475–8. http://dx.doi.org/10.1002/cjce.5450520407.
[19] Poulikakos D. Thermal instability in a horizontal fluid layer superposed on a heat-generating porous bed. Numer Heat Transfer 1987;12:83–99. http://dx.doi.org/10.1080/10407788708913575.
[20] Vafai K, Kim SJ. Fluid mechanics of the interface region between a porous medium and a fluid layer, an exact solution. Int J Heat Fluid Flow 1990;11:254–6. http://dx.doi.org/10.1016/0142-727X(90)90045-D.
[21] Ochoa-Tapia JA, Whitaker S. Momentum transfer at the boundary between a porous medium and a homogeneous fluid-II. comparison with experiment. Int J Heat Mass Transfer 1995;38:2647–55. http://dx.doi.org/10.1016/0017-9310(94)00347-X.
[22] Chandesris M, Jamet D. Boundary conditions at a planar fluid-porous interface for a poiseuille flow. Int J Heat Mass Transfer 2006;49:2137–50. http://dx.doi.org/10.1016/j.ijheatmasstransfer.2005.12.010.
[23] Valdés-Parada F, Alvarez-Ramirez J, Goyeau B, Ochoa-Tapia J. Computation of jump coefficients for momentum transfer between a porous medium and a fluid using a closed generalized transfer equation. Transp Porous Media 2009;78:439–57. http://dx.doi.org/10.1007/s11242-009-9370-9.
[24] Wood B. The role of scaling laws in upscaling. Adv Water Resour 2009;32:723–36. http://dx.doi.org/10.1016/j.advwatres.2008.08.015.
[25] Wood B, Valdés-Parada F. Volume averaging: local and nonlocal closures using a Green's function approach. Adv Water Resour 2013;51:139–67. http://dx.doi.org/10.1016/j.advwatres.2012.06.008.
[26] Aguilar-Madera C, Valdés-Parada F, Goyeau B, Ochoa-Tapia J. Convective heat transfer in a channel partially filled with a porous medium. Int J Thermal Sci 2011;50:1355–68. http://dx.doi.org/10.1016/j.ijthermalsci.2011.03.005.
[27] Haberman R. Applied partial differential equations with fourier series and boundary value problems. fifth ed. Pearson; 2012.